Available online at www.sciencedirect.com
SCIENCE DIRECT
Catalysis Today 116 (2006) 384–390
CATALYSIS TODAY
www.elsevier.com/locate/cattod

Physico-chemical properties and reactivity of Au/CeO_2 catalysts in total and selective oxidation of CO

F. Arena [a,b,*], P. Famulari [a], N. Interdonato [a], G. Bonura [b], F. Frusteri [b], L. Spadaro [b]

[a] *Dipartimento di Chimica Industriale e Ingegneria dei Materiali, Università degli Studi di Messina, Salita Sperone 31, I-98166 S. Agata (Messina), Italy*
[b] *Istituto CNR-ITAE "Nicola Giordano", Salita S. Lucia 39, 98126 S. Lucia (Messina), Italy*

Available online 10 July 2006

Abstract

The effects of the preparation method (deposition–precipitation, incipient-wetness, combustion) on the structure and redox properties of 1% Au/CeO_2 catalyst have been probed by TPR, XRD, and TEM techniques. The catalytic pattern in total (COX) and selective (SCOX) CO oxidation has been assessed by temperature programmed reaction tests in the range 273–473 K. Controlling residual chlorine, the synthesis route determines the strength of the Au–CeO_2 interaction which affects both the reduction of the active phase and the CO oxidation functionality. Removal of chlorine by washing in a diluted alkaline solution enables then an easy reduction of Au precursor levelling off the reactivity of the Au/CeO_2 catalysts.

Keywords: Au/CeO_2 catalyst; Preparation method; Total and selective CO oxidation; Chlorine effect

1. Introduction

For long time considered as a catalytically inactive material because of its chemical inertness towards almost all the elements and compounds [1], the last decades witnessed a rapid growth of research interest on supported gold catalysts as, contrarily to bulk metal, these effectively drive various catalytic reactions [2–21]. In particular, a superior reactivity in low temperature CO oxidation and WGS processes has been generally ascertained [2–8,11–21].

The stabilization of Au clusters with an optimum diameter of 2–3 nm is an essential requirement for attaining active catalysts [2,5–8], as nanosized metal particles do not exhibit conventional noble behaviour [1–7] denoting instead a peculiar reactivity towards oxygen, hydrogen, water and carbon monoxide molecules, due to some specific active centres at the Au^0/support interface [2–9,18–21].

Deposition–precipitation, co-precipitation and phosphine-grafting are recommended synthesis routes, whilst conventional impregnation techniques generally lead to poorly active systems [2,5–7,11–21]. Carrier also plays a crucial role, as semiconducting oxides, mostly Fe_2O_3 and TiO_2, confer a higher reactivity to Au catalysts [2–7]. Indeed, providing fairly active oxygen species reducible oxide carriers could overcome the particle size effect in CO oxidation [2–7,18–21].

Although a peculiar reactivity of ceria confers a unique reactivity to supported phases [22], few reports have been till now devoted to the physico-chemical and catalytic features of the Au/CeO_2 system [12,13,15–17,21].

Therefore, this study is aimed at assessing the effects of the preparation method on the activity pattern of 1 wt.% Au/CeO_2 catalysts in the oxidation of CO, in presence (SCOX) and absence of hydrogen (COX), highlighting some meaningful relationships amongst chemical composition, redox and catalytic properties of the system.

2. Experimental

2.1. Catalyst preparation

Supported Au/CeO_2 (1 wt.% Au) catalysts were prepared by deposition–precipitation (DP), incipient-wetness (IW) and combustion (CB) [12] routes using the $HAuCl_4{\cdot}3H_2O$ precursor (Carlo Erba, purity >99%).

The list of the catalysts along with relative notation, Au loading (as evaluated by XRF analysis), SA_{BET} values and amount of residual Cl, is presented in Table 1.

* Corresponding author.
E-mail address: Francesco.Arena@unime.it (F. Arena).

0920-5861/$ – see front matter © 2006 Elsevier B.V. All rights reserved.
doi:10.1016/j.cattod.2006.05.082

Table 1
List of the samples

Code	Preparation method	Au loading (wt.%)	SA_{BET} (m^2/g)	[Cl] (wt.%)	Cl_{at}/Au_{at}
CeO_2	Combustion	–	44	–	–
CB	Combustion	0.85	30	0.27	1.9
DP	Deposition–precipitation	1.00	35	–	0.0
IW	Incipient-wetness	1.00	50	0.68	3.8

2.2. Washing treatment and quantitative analysis of chlorine

A CB catalyst sample (≈3 g) was dispersed into a 50 ml NaOH aqueous solution (pH ≈ 9) at 343 K under stirring. The solution resulting from three extractions (≈150 ml) was used for analysis of chloride by the Volhard method, while the solid (CB-w) was washed with water and dried at 373 K (16 h).

2.3. TEM characterisation

TEM characterisation was performed by a Philips CM12 transmission electron microscope on powder samples deposited on a copper grid, coated with a porous carbon film.

2.4. X-ray diffraction (XRD)

X-ray diffraction (XRD) spectra were obtained by an APD-2000 diffractometer (Ital-Structures) operated at 40 kV and 30 mA, employing a Ni-filtered Cu Kα radiation (λ = 1.5406 Å). Identification of peaks was made on the basis of the JCPDS database [23].

2.5. Temperature programmed reduction (TPR)

Temperature programmed reduction (TPR) measurements in the range 293–1073 K were performed using a 6% H_2/Ar reducing mixture carrier flowing at 60 STP ml min^{-1}. The experiments were carried out with a heating rate of 12 K min^{-1} and an Au load of ca. 1.0 mg.

2.6. Catalyst testing

Catalyst testing in the CO oxidation reaction, in absence (COX) and presence of hydrogen (SCOX), were performed by temperature programmed reaction tests [24], using a linear quartz reactor (i.d., 4 mm) connected on line to a quadrupole mass spectrometer (Thermolab, Fisons Instruments) for continuous scanning of the reaction stream. Tests were run in the range 273–473 K using 0.02 g of catalyst diluted with 0.15 g of powdered SiC, a heating rate of 4 K min^{-1} and reaction mixtures in the molar ratios $CO:O_2:He = 2:2:96$ (COX) and $CO:O_2:H_2:He = 1:2:50:47$ (SCOX) flowing at 50 and 100 STP ml min^{-1}, respectively. Taking helium as internal standard, CO and H_2 conversion values obtained by the mass balance were always in a satisfactory agreement (±10%) with those obtained by the internal standard method. The kinetic constant values from a pseudo-first order integral equation were used for the Arrhenius plot correlations of CO and H_2 oxidation, considering always conversion values below 25%.

3. Results

3.1. Redox behaviour

The TPR pattern in the range 293–1073 K of the CeO_2 carrier and catalysts obtained by the different synthesis routes are shown in Fig. 1. While the onset temperature of reduction ($T_{o,red}$), the temperature of peak maximum (T_{Mi}) and the extent

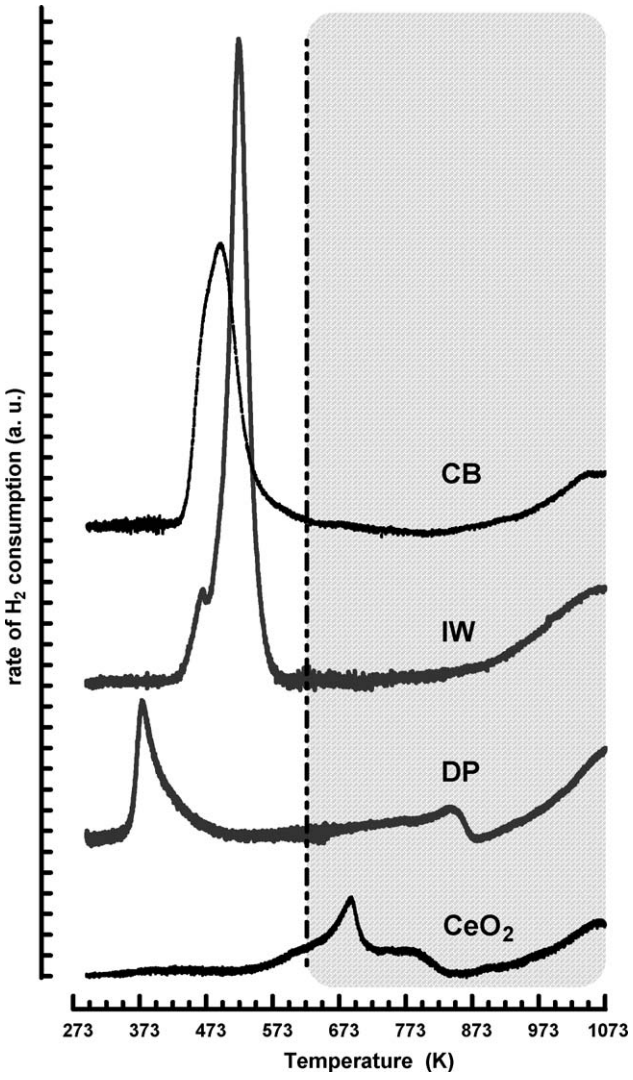

Fig. 1. Effect of the preparation method on the TPR profiles of the ‘‘untreated’’ DP, CB and IW catalysts.

Table 2
TPR data of Au/CeO_2 catalysts

Sample	$T_{o,red}$ (K)	T_{M1} (K)	T_{M2} (K)	H_2 consumption		
				($\mu mol/g_{cat}$)[a]	H_2/Au[b]	$[Ce^{III}/Ce^{IV}]$[a]
CeO_2	504	692	–	637	–	0.22
DP	345	376	–	812	6.1	0.27
IW	423	522	–	1764	23.9	0.65
CB	421	495	1052	1173	21.3	0.38
CB-w	300	460	1063	767	12.2	0.24

Effect of preparation method and washing treatment.
[a] In the range 273–1073K.
[b] In the range 273–623 K.

of H_2 consumption, expressed both as mole per weight unit in the full range 273–1073 K and number of H_2 molecules consumed per Au atom (T range, 293–623 K), are summarised in Table 2.

The TPR pattern of the ceria matrix features a typical profile arising from the reduction of Ce^{IV} ions at the surface (peak at ca. 700 K) and then in the bulk [13,16,22], whose integral area (273–1073 K) corresponds to an average degree of reduction of ca. 22%.

The reduction profile of all the catalysts consists of one main peak centred between 375 and 500 K whose intensity, shape and position depend strongly on the synthesis route, while at $T > 873$ K all the catalysts feature a trend of reduction comparable with that of ceria support.

The DP catalyst features the easiest reducibility evidenced by the lowest $T_{o,red}$ (345 K) and T_{M1} (376 K) values, while a relatively ''low'' H_2 consumption corresponds to a H_2/Au ratio equal to 6.1, anyhow quite larger than the stoichiometric consumption (1.5) of the Au precursor. According to the highest $T_{o,red}$ (423 K) and T_{M1} (522 K) values, the IW is the less reducible system, though a much larger intensity of the main peak (1244 μmol/g) accounts for the largest hydrogen consumption and H_2/Au ratio value (23.9). A very small though resolved component on the low temperature side of the main peak signals an easy reduction of a minor fraction of Au ions. At least, the CB sample displays a reduction pattern characterised by a ''broad'' peak with a similar $T_{o,red}$ (421 K), but centred at a lower temperature (495 K), the intensity (929 μmol/g) of which signals a H_2/Au ratio (21.3) close to that of the IW sample.

Such reduction patterns mirror the peculiar characteristics of the relative synthesis route:

(a) the DP catalyst obtained using a ''pre-shaped'' carrier and ''free'' from residual chlorine;
(b) the CB catalyst prepared forming both support and active phase by a solid-state reaction at ca. 1273 K [12,22] and containing a fraction of residual chlorine (Cl_{at}/Au_{at}, 1.9);
(c) the IW catalyst obtained from a ''pre-shaped'' carrier and bearing the ''undecomposed'' Au precursor ($Cl_{at}/Au_{at} \approx 4$) [18].

Deposition–precipitation (a) and incipient-wetness (c), though involving a ''pre-shaped'' carrier of which they keep practically unchanged the physical features (Table 1), represent the opposite ends with the lowest and largest amount of residual chlorine, accounting for the easiest and hardest reducibility, respectively. ''Building'' the catalyst structure by a violent

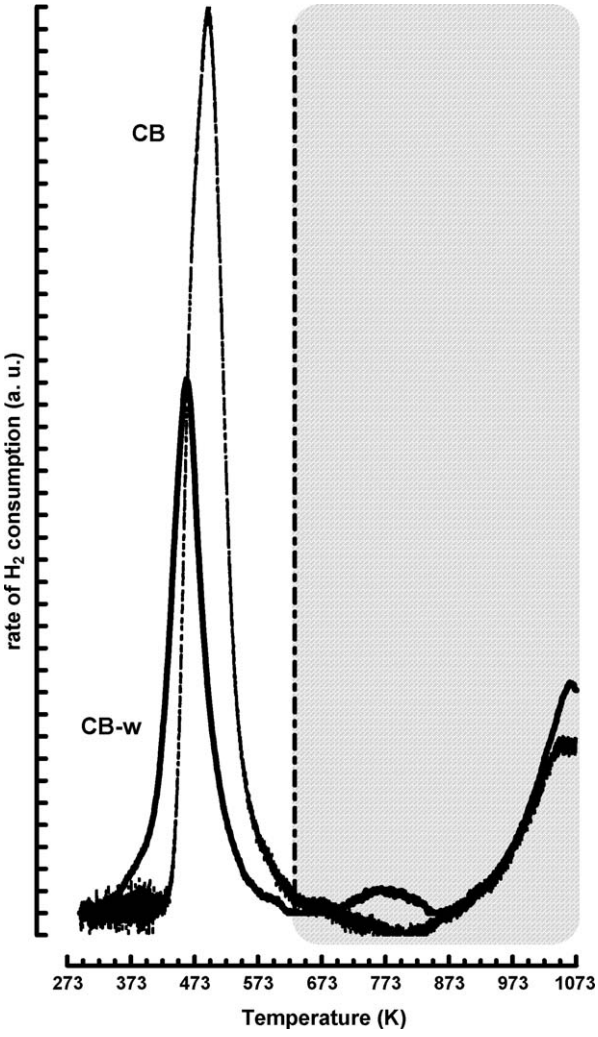

Fig. 2. Effect of the washing treatment (CB-w) on the TPR profile of the CB catalyst.

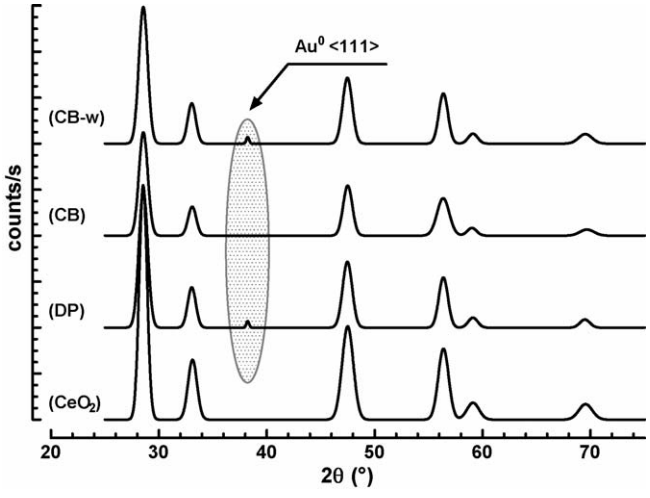

Fig. 3. XRD patterns of CeO_2 and Au/CeO_2 catalysts.

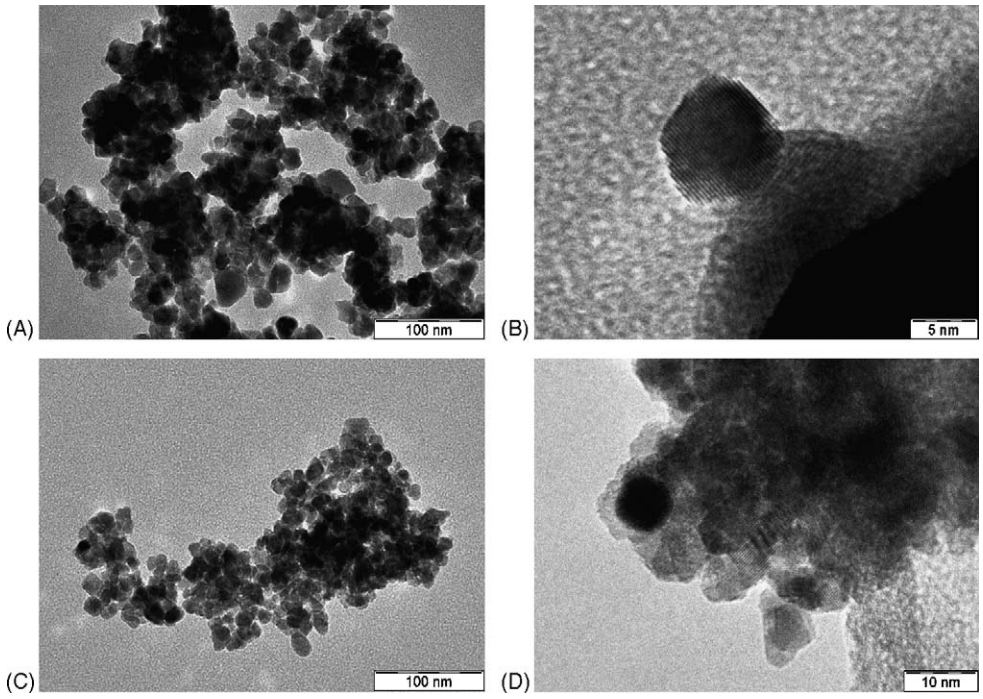

Fig. 4. TEM images of the DP (A and B) and CB-w (C and D) catalysts at different magnifications.

redox reaction of precursors with urea, implies a partial decomposition of the Au precursor and a shift of both $T_{o,red}$ and T_{M1} upward by ca. 80 and 110 K with respect to DP.

The effect of chlorine elimination on the reduction pattern of the CB system is shown in Fig. 2, while the characteristic temperatures and the H_2 consumption of the CB-w sample are included in Table 2. Removal of chlorine enhances the reducibility of the active phase with respect to the ''untreated'' CB sample, evidenced by a downward shift of $T_{o,red}$ and T_{M1} by ca. 120 and 35 K, respectively. Besides, an evident decrease of the H_2 consumption (Fig. 2) results in a halved (12.2) H_2/Au ratio.

3.2. Structural properties

The XRD patterns of the ceria support, of the ''untreated'' and ''washed'' samples are shown in Fig. 3. All spectra display

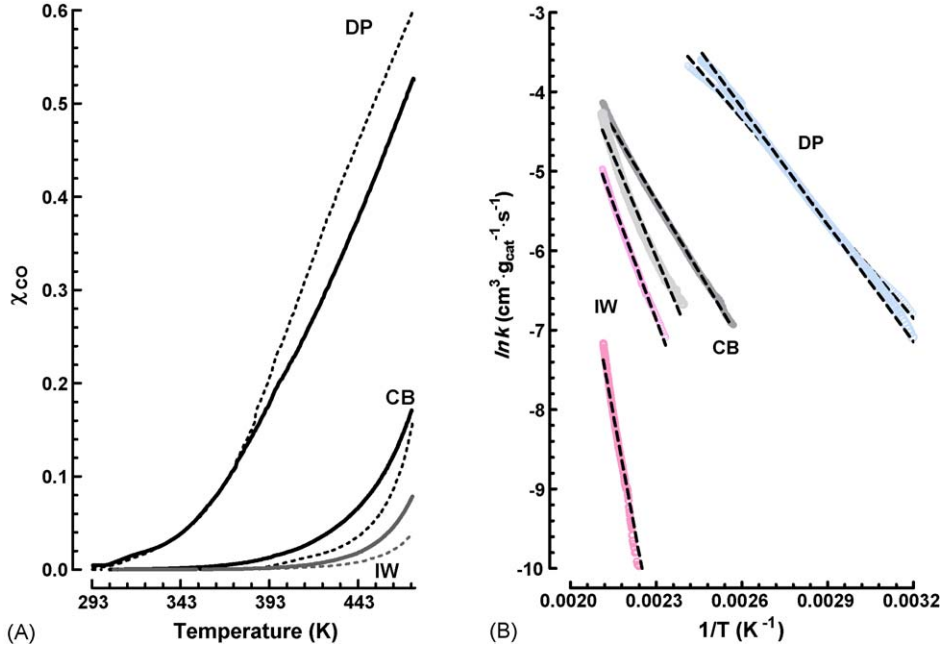

Fig. 5. COX activity data of the ''untreated'' DP, CB and IW catalysts in the 1st (dotted lines) and subsequent (2nd–4th) reaction cycles (solid lines) in the range 273–473 K. (A) CO conversion *vs*. *T* and (B) Arrhenius plots in the CO conversion range 1–25%.

Table 3
COX reaction

Catalyst	1st run			2nd–4th run		
	T range (K)	R^2	E_{app} (kcal/mol)	T range (K)	R^2	E_{app} (kcal/mol)
DP	313–409	0.994	10	314–416	0.998	10
CB	428–473	0.979	27	389–470	0.999	12
IW	435–474	0.990	39	428–474	0.997	19

Activation energy data in 1st and 2nd–4th runs.

the typical diffraction lines of the cerianite with a fluorite-like structure, an additional reflex at 38.19°, characteristic of metallic Au (e.g., ⟨1 1 1⟩ plane) [13,23], being evident for the DP and CB-w samples.

TEM pictures (Fig. 4) of DP (A and B) and CB-w (C and D) samples at different magnifications display large agglomerated of small (10–20 nm) ceria particles where Au particles are hardly discernible. Rather ''smoothed'' Au particles ''sunk'' in the ceria structure with a variable size diameter (7–10 nm) are observable on both catalysts at higher magnification.

3.3. Catalyst activity in CO total (COX) and selective (SCOX) oxidation

Catalytic data in the COX reaction of the ''untreated'' catalysts, in terms of CO conversion with T (A) and Arrhenius plots (B), are shown in Fig. 5. Marked differences in both the onset temperature of CO oxidation ($T_{o,CO}$) and final (473 K) conversion values spanning from DP to IW preparation methods are evident. With the lowest $T_{o,CO}$ (300 K) and a final conversion of ca. 60% at 473 K, the DP catalyst results the most active system. The performance of the IW and CB samples is much poorer, according to considerably higher ignition temperatures ($T_{o,CO}$, ≈390 K) and final (at 473 K) conversion values of only ca. 4 and 7%, respectively. The Arrhenius plots (Fig. 5B) depict fairly reliable straight-line relationships ($r^2 > 0.97$) resulting in E_{app} values (Table 3) comprised between 10 (DP) and 39 kcal/mol (IW), in agreement with the activity scale from $T_{o,CO}$ and final X_{CO} values.

In order to rule out the influence of potential activation–deactivation phenomena, all the catalysts were then subjected to four consecutive reaction cycles. After significant changes from 1st (dotted lines) to the 2nd run, the activity kept practically unchanged until the 4th run (solid lines), which has been taken as reference stationary activity level. The DP catalyst displays no changes in activity up to 373 K and only a slight decrease in activity at $T > 373$ K resulting in an unchanged (10 kcal/mol) E_{app} value. A downward shift of $T_{o,CO}$ (300 K) by ca. 100 K mirrors a much higher reactivity of CB and IW systems, attaining final X_{CO} value of ca. 15 and 8% which correspond to E_{app} values equal to 12 and 19 kcal/mol, respectively.

Referred to the preparation method, these data result in the following activity scale:

$$DP \gg CB > IW.$$

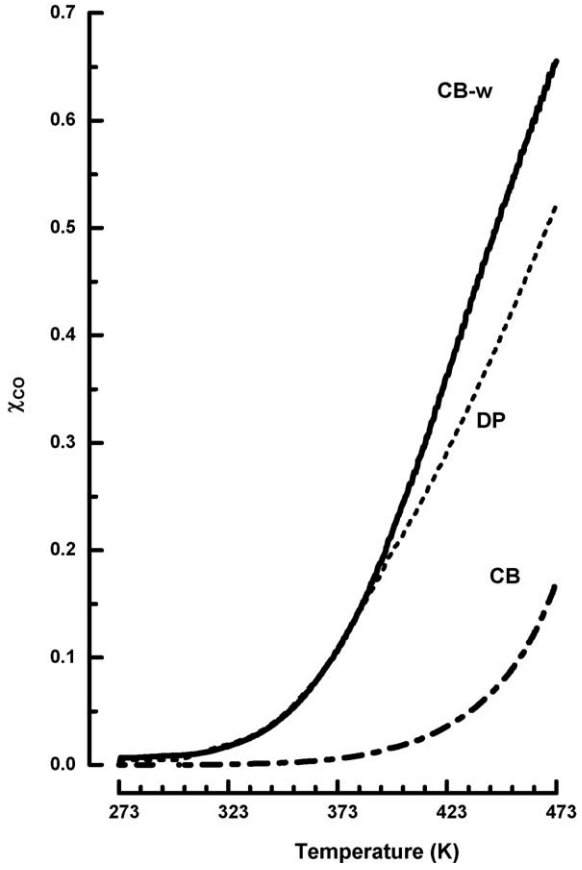

Fig. 6. COX ''stationary'' activity data of the CB-w catalyst in the range 273–473 K.

The effects of chlorine elimination are evident from the comparison of the ''stationary'' activity (4th run) of the CB and CB-w catalysts. The trend of X_{CO} with temperature (A) and the relative Arrhenius plots (B) are compared in Fig. 6, while the E_{app} data are summarised in Table 4. It is evident that removal of ''residual'' chlorine levels off the COX functionality with respect to the preparation method, enabling a catalytic pattern

Table 4
COX reaction

Catalyst	$d_{Au,\ XRD}$ (nm)	Temperature range (K)	R^2	E_{app} (kcal/mol)
CB-w	8	325–394	0.999	10
DP	11	314–416	0.998	10

Arrhenius plot data of the CB-w and DP catalysts.

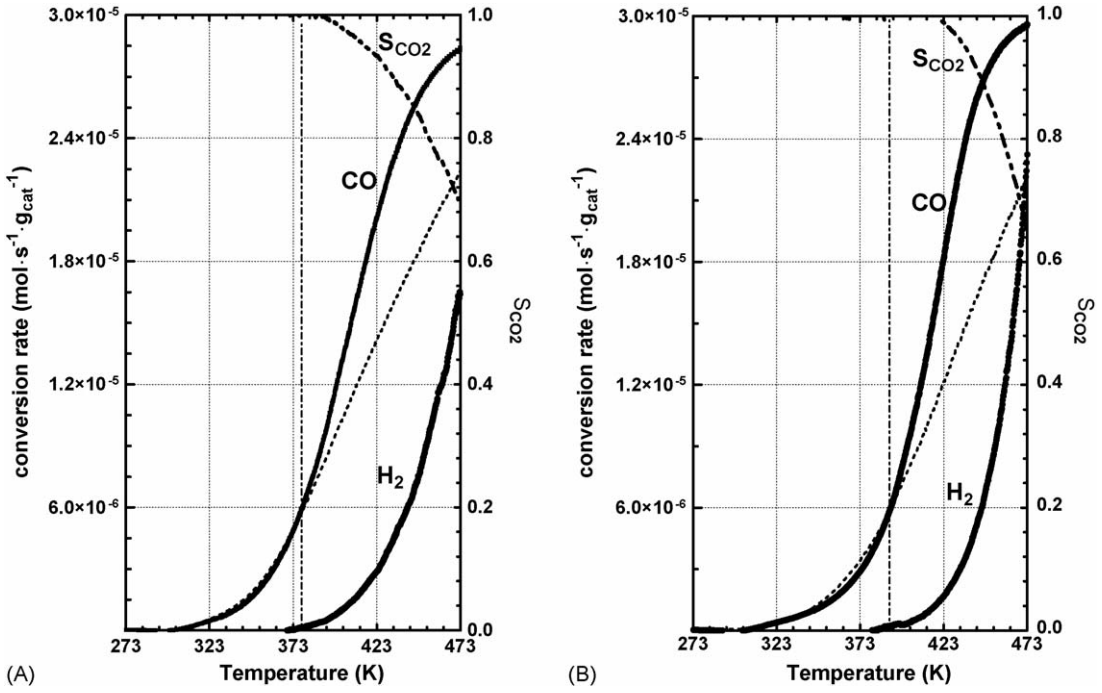

Fig. 7. SCOX activity data of the DP (A) and CB-w (B) catalyst in the range 273–473 K.

comparable or even superior to that of the DP system as also confirmed by the same E_{app} value (10 kcal/mol).

Finally, the reactivity of the DP (A) and CB-w (B) catalysts in the SCOX reaction is compared in Fig. 7, showing both the CO and H_2 conversion rates as a function of temperature. Both catalysts display an analogous behaviour pattern also in the SCOX reaction with a CO conversion rate practically unaffected by the presence of H_2 up to 380–400 K, when the formation of water starts. Thereafter, an increasing rate of H_2 oxidation leads to a regular decrease in the S_{CO_2} from 100% to ca. 75 and 65% at 473 on the former and latter systems, respectively, while, in concomitance with water formation, the rate of CO conversion rises much more steeply than in absence of hydrogen. These data mirror an unchanged E_{app} value for CO oxidation (10 kcal/mol), while that of the H_2 oxidation results higher on both systems going from 14 (DP) to 19 (CB-w) kcal/mol.

4. Discussion

4.1. Structure and redox properties

Different synthesis routes involving wide ranges of residual chlorine (Cl_{at}/Au_{at}, 0–3.8) have been adopted in order to highlight its main effects on the physico-chemical and catalytic properties of the Au/CeO_2 system. Unlikely a reliable assessment of metal dispersion is not straightforward owing to the failure of chemisorption methods [2–7] while, in a qualitative agreement with TEM evidences (Fig. 4), XRD analyses stress the contribution of large crystalline Au particles [12,13,16,18] providing an average estimate of the metal particle size of 8–11 nm (Table 4). Although this range would exceed the optimum size indicated for an effective catalytic functionality [2–8], both the DP and CB-w systems exhibit indeed a reactivity comparable with that of very active catalysts [18,20]. In this respect, it must be stressed that some authors argued that the catalytic activity could arise from a low concentration of extremely active specific sites, questioning the absolute validity of dispersion as a key-parameter for predicting the reactivity of the Au systems [13,16,20].

The peculiar solid-state reactivity of ceria-based systems, yet, allows to get indirect information on the relative dispersion of the supported species from a synergetic effect on the reduction of surface Ce^{IV} ions at temperatures lower than those of the bare ceria (e.g., 700–800 K) [12,13,16,22]. Thus, the reduction of the ceria carrier in concomitance with that of the active phase [13,16,22] will result in H_2/Au values (Table 2) increasing with the dispersion of Au^{3+} ions [13,16,22]. Pointing to a strong promoting effect on the reduction of the ceria matrix [12,13,16] hence, the hard reduction and the very large values of the H_2/Au ratio of the "Cl-containing" CB and IW catalysts (Table 2) prove that the strength of the "Au^{3+}–CeO_2" interaction parallels the enhanced dispersion of the precursor, mediated by a high affinity of chloride for Au^{3+} ions [18,20] and ceria lattice [22]. The formation of the CeOCl phase [22] during reduction likely explains the enhanced reducibility of Ce^{IV} ions in "Cl-containing" systems.

Accordingly, easier reduction and "lower" H_2/Au ratios of the "Cl-free" DP and CB-w samples confirm that in absence of "residual" chlorine the formation of fairly reactive gold oxo-complexes leads to a considerable weakening of the Au–CeO_2 interaction [2–8,18,20].

4.2. Structure–activity relationships

With the exception of the DP catalyst which, characterised by the presence of metallic Au (Fig. 3), displays a

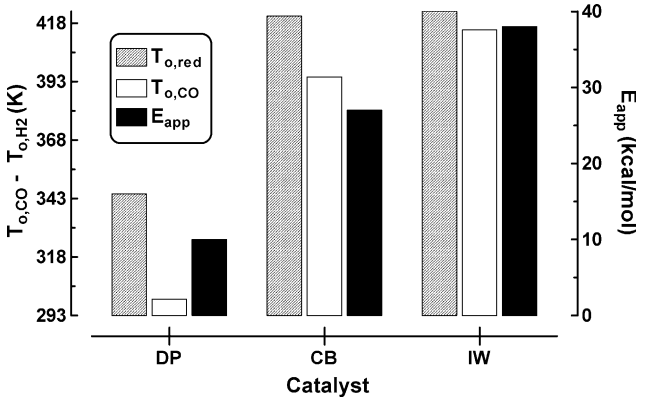

Fig. 8. Comparison of $T_{o,red}$ (Table 2), $T_{o,CO}$ and E_{app} values for the "untreated" DP, CB and IW catalysts in the 1st reaction cycle (Fig. 5).

considerable COX activity still in the 1st cycle (Fig. 5), the poor catalytic performance of the "untreated" CB and IW catalysts is evidently attributable to a substantial lack of active sites, somewhat associated with the absence of metal particles [18,20]. Indeed, a hard reducibility of "Cl-containing" catalysts (Fig. 1) hinders the generation of active Au^0/Au^+ sites at the metal/support interface and consequently the CO oxidation functionality [18,20]. Then, higher $T_{o,red}$ parallel higher $T_{o,CO}$ and E_{app} values (Fig. 8) indicating that for the "untreated" catalysts the Au^{3+} reduction accounts for unusually high values of the energetic barrier (27–39 kcal/mol) [12,18]. Anyway, a higher reactivity of the Au/CeO_2 system towards CO rather than hydrogen is evident from systematically lower $T_{o,CO}$ values (Fig. 8).

The downward shift of the ignition temperature coupled to a consequent improvement of the COX activity at stationary conditions (Fig. 5) indicates that a small fraction of active sites is generated during the first reaction cycle, though the "toxic" effect of chlorine keeps low the overall activity level [2–4,18,20]. Due to a marked enhancement of the Au reducibility (Fig. 2), a complete elimination of chlorine levels off any further difference in catalytic activity [18,20].

Therefore, despite of a mean Au particles size estimate (Table 4) out of the optimum range for catalytic activity, the high performance of the studied systems [2–5,18–21] confirms that the dispersion is not the sole parameter accounting for the catalytic behaviour of the Au/CeO_2 system. Likely, the peculiar reactivity of the ceria carrier concurs to enhance the influence of the metal particles morphology on the CO oxidation functionality [18–21]. Anyhow, because of a more pronounced reactivity of the Au/CeO_2 system towards CO (Fig. 8), both the CB-w and DP catalysts exhibit a full CO_2 selectivity up to ca. 380 K, deserving a potential application in low-temperature fuel cell devices [21]. The enhanced rate of CO conversion at $T > 400$ K in presence of hydrogen would be consequent to the formation of water likely driving a parallel WGS reaction pathway [13,16,17]. Perhaps, the stabilization of "Au^+–OH" species at the metal–oxide interface could concur to drive a more effective CO oxidation path [2–4,6–8,10].

5. Conclusions

The main findings of this work can be summarised into the following main items:

- Controlling the amount of residual chlorine, the preparation method determines the strength of the Au–CeO_2 interaction.
- Affecting catalyst reducibility and the consequent generation of active sites, the preparation method controls also the CO oxidation functionality.
- Removal of residual chlorine by washing treatment in alkaline solution enhances the reducibility of the active phase levelling off the catalytic functionality of Au/CeO_2 system with reference to the preparation method in both COX and SCOX reactions.
- The Au/CeO_2 system is a superior catalyst for "total" and "selective" oxidation of CO, deserving potential applications in low-temperature fuel cells devices.

References

[1] B. Hammer, J.K. Norskov, Nature 376 (1995) 238.
[2] M. Haruta, Catal. Today 36 (1997) 153.
[3] M. Haruta, M. Daté, Appl. Catal. A 222 (2001) 427.
[4] M. Haruta, CATTECH 6 (2002) 102.
[5] A.I. Kozlov, A.P. Kozlova, H. Liu, Y. Iwasawa, Appl. Catal. A 182 (1999) 9.
[6] G.C. Bond, D.T. Thompson, Gold Bull. 33 (2000) 41.
[7] G.C. Bond, D.T. Thompson, Catal. Rev.-Sci. Eng. 41 (1999) 319.
[8] D.T. Thompson, Appl. Catal. A 243 (2003) 201.
[9] R. Meyer, C. Lemire, Sh.K. Shaikhutdinov, H.-J. Freund, Gold Bull. 37 (2004) 72.
[10] A. Ueda, M. Haruta, Gold Bull. 32 (1999) 3.
[11] A. Wolf, F. Schüth, Appl. Catal. A 226 (2002) 1.
[12] P. Bera, M.S. Hegdé, Catal. Lett. 79 (2002) 75.
[13] Q. Fu, M. Flytzani-Stephanopoulos, Catal. Lett. 77 (2001) 87.
[14] S.D. Lin, M. Bollinger, M.A. Vannice, Catal. Lett. 17 (1993) 245.
[15] E.A. Shaw, A.P. Walker, T. Rayment, R.M. Lambert, J. Catal. 134 (1992) 747.
[16] Q. Fu, S. Kudriavtseva, H. Saltsburg, M. Flytzani-Stephanopoulos, Chem. Eng. J. 93 (2003) 41.
[17] T. Tabakova, F. Boccuzzi, M. Manzoli, J.W. Sobczak, V. Idakiev, D. Andreeva, Appl. Catal. B: Environ. 49 (2004) 73.
[18] J.M.C. Soares, P. Morrall, A. Crossley, P. Harris, M. Bowker, J. Catal. 219 (2003) 17.
[19] R.J.H. Grisel, B.E. Nieuwenhuys, J. Catal. 199 (2001) 48.
[20] H.-S. Oh, J.H. Yang, C.K. Costello, Y.M. Wang, S.R. Bare, H.H. Kung, M.C. Kung, J. Catal. 210 (2002) 375.
[21] S. Carrettin, P. Concepción, A. Corma, J.M. López Nieto, V.F. Puntes, Angew. Chem. Int. Ed. 43 (2004) 2538.
[22] A. Trovarelli, Catalysis by Ceria and Related Materials, Imperial College Press, London, 2002.
[23] Joint Committee Powder Diffraction System, International Centre for Diffraction Data, Swarthmore, USA, 1983.
[24] F. Arena, F. Frusteri, A. Parmaliana, N. Giordano, Appl. Catal. A 125 (1995) 39.